Astron. Astrophys. 335, 894–898 (1998)

ASTRONOMY AND ASTROPHYSICS

Research Note

The effective velocity and radius of spiral galaxies

L. Vertchenko[1,2] **and R.J. Quiroga**[2]

[1] Departamento de Física e Química, PUC-MG, Caixa Postal 1686, 30.535-610 Belo Horizonte MG, Brazil
[2] Departamento de Física, UFMG, Caixa Postal 702, 30.161-970 Belo Horizonte MG, Brazil

Received 29 November 1997 / Accepted 14 April 1998

Abstract. The averaged radius and velocity respectively associated to global potential and kinetic energies, are computed for spiral galaxies. Such dynamical parameters (effective radius and velocity) can be directly related to observational ones, being $R_{\rm eff} \approx R_{\rm lim}$ and $V_{\rm eff} \approx v_{\omega,\rm lim}$, where $R_{\rm lim}$ is either the R_{25} radius or the last observed point of the rotation curve of the galaxy and $v_{\omega,\rm lim}$ is its rotational velocity at this radius. It is proposed that the angular momentum can be replaced by the *action*, $A = MR_{\rm eff}V_{\rm eff}$, in the study of dynamical characterization of spiral galaxies (see, for instance, the analysis of Campos-Aguilar et al. (1993)).

Key words: galaxies: spiral – galaxies: fundamental parameters

1. Our proposition

The search for fundamental parameters of spiral galaxies involves their analysis in dynamical parametrical planes. Here we use Begeman's (1987) models of spiral galaxies to deduce a direct correspondence between the pair of observational parameters (limit radius, rotational velocity) and the pair of dynamical ones ($R_{\rm eff}$, $V_{\rm eff}$), being $R_{\rm eff}$ and $V_{\rm eff}$ the averaged radius and velocity respectively associated to global potential and kinetic energies. It is proposed the association of these parameters with the integral parameter "action", whose significance we examine in the context of Jacobi dynamics.

2. Effective velocity and radius

$V_{\rm eff}$ and $R_{\rm eff}$ are associated to global kinetic and potential energies through

$$V_{\rm eff} = \left(\frac{2E_{\rm K}}{M}\right)^{\frac{1}{2}} \tag{1}$$

and

$$R_{\rm eff} = \frac{GM^2}{|E_{\rm P}|}. \tag{2}$$

Send offprint requests to: L. Vertchenko at address 1

Using high quality rotational curves, Begeman (1987) decomposed eight spiral galaxies in a dark halo of mass distribution

$$\rho(r) = \frac{\rho_0}{1+(r/a)^2} \tag{3}$$

and in visible components: an exponential stellar disk of non-zero thickness (Casertano 1983), a gaseous disk and, for three galaxies, a bulge. For these galaxies we employ his decomposition to compute $E_{\rm P}$ inside spheres of radius $R_{\rm lim}$ given by the photometric radius R_{25} as well as the last observed point in the rotational curve. However, in our calculations we simplify the visible components using a zero-thickness exponential disk[1] of scale-length h and, for galaxies which have a bulge, a Hernquist sphere (Hernquist 1990). For two of these galaxies (NGC 2841 and NGC 7331) we truncated the Hernquist sphere to be in accordance with the truncated photometric curves of their bulges (Begeman 1987). The values for the parameters of halo, disk mass and scale-length and bulge mass were the same of Begeman (1987), while the characteristic length of Hernquist spheres was obtained by fitting their circular velocities to values listed for the bulges.

The radial distribution of neutral hydrogen of four galaxies was taken from the plots of Begeman (1987) and used to do a slight correction in their disk surface density, which becomes

$$\Sigma_{\rm d}(R) = \Sigma_0 \exp(-R/h) + 1.4\Sigma_{\rm H}(R), \tag{4}$$

where the factor 1.4 is due to the presence of He. In these cases, the sphere used for the calculation of $R_{\rm eff}$ was limited by the eye-estimated point wherein the $\Sigma_{\rm H}$ becomes null in Begeman's (1987) figures.

The expressions used in computing the potential energy, which is necessary to obtain $R_{\rm eff}$ by Eq. (2), are presented in the Appendix A. We assume that the galaxies satisfy the virial global-equilibrium condition and therefore, once their

[1] We have verified that the substitution of Casertano (1983) disk by the zero-thickness exponential disk does not alter significantly the total disk mass in the process of fitting observed velocities to the model rotational curves.

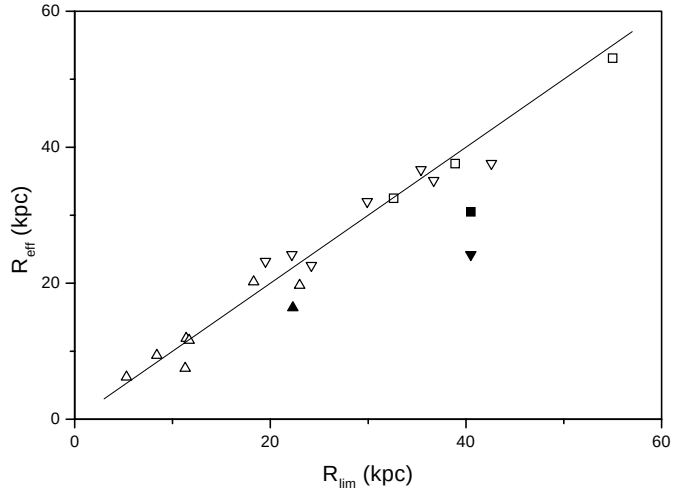

Fig. 1. $R_{\rm eff}$ vs. $R_{\rm lim}$ for the data of Table 1. The symbols $\triangle$, ∇, and $\square$ refer, respectively, to the first, second and third rows for each galaxy in the table. The full symbols are related to NGC 5371. The line corresponds to $R_{\rm eff} = R_{\rm lim}$.

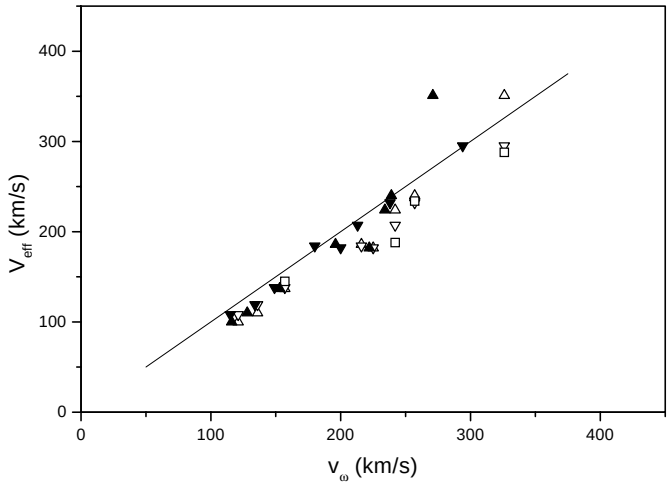

Fig. 2. $V_{\rm eff}$ vs. $v_{\omega,\rm max}$ (empty symbols) and $v_{\omega,\rm lim}$ (filled symbols). The up triangle, down triangle and square refer, respectively, to the first, second and third rows for each galaxy in Table 1. The line is $V_{\rm eff} = v_{\omega,\rm max} = v_{\omega,\rm lim}$.

$R_{\rm eff}$ and mass have been calculated, the $V_{\rm eff}$ can be easily obtained through

$$V_{\rm eff} = \left(\frac{GM}{R_{\rm eff}}\right)^{\frac{1}{2}}. \quad (5)$$

For simplicity, we assume that the stellar disk follows the gas in its rotation. If the rotational kinetic energy of the galactic disk,

$$E_\omega = \pi \int \Sigma_{\rm d} v_\omega^2 R \, {\rm dR} \quad (6)$$

represents the main part of the global rotation of a spiral galaxy, one can also estimate the ratio between rotational and total kinetic energy, ξ.

In Table 1 we list, for the eight galaxies of Begeman (1987), the values of $V_{\rm eff}$, $R_{\rm eff}$, ξ, the limit-radius $R_{\rm lim}$ used in the calculations and the observed $v_{\omega,\rm max}$ and $v_{\omega,\rm lim} = v_\omega(R_{\rm lim})$.

In Figs. 1 and 2 the plots of $R_{\rm eff}$ vs. $R_{\rm lim}$ and $V_{\rm eff}$ vs. $v_{\omega,\rm max}$ and $v_{\omega,\rm lim}$ are presented. They allow us to conclude that

$$R_{\rm eff} \approx R_{\rm lim} \quad (7)$$

and

$$V_{\rm eff} \approx v_{\omega,\rm lim} \quad (8)$$

for the galaxies of Table 1. The unique exceptions are two $R_{\rm eff}$ data-points calculated with $R_{\rm lim} > R_{25}$ for NGC 5371, which does not need a halo in the best-fit Begeman (1987) model.

Table 1. Effective radius and velocity, rotational fraction of kinetic energy, limit-radius used in calculations, rotational velocity at the limit-radius and maximum of rotational velocity for Begeman's (1987) sample of spiral galaxies. For each galaxy, in the first row $R_{\rm lim} = R_{25}$; in the second row $R_{\rm lim}$ corresponds to the last observed point in rotational curve and in the third row of galaxies NGC 3198, NCG 7331, NCG 2841 and NCG 5371 $R_{\rm lim}$ marks the point wherein $\Sigma_{\rm H}$ becomes null in Eq. (4).

NGC	$R_{\rm eff}$	$V_{\rm eff}$	ξ	$R_{\rm lim}$	$v_{\omega,\rm lim}$	$v_{\omega,\rm max}$
type	(kpc)	(km/s)		(kpc)	(km/s)	(km/s)
3198	11.9	137	0.54	11.4	153	157
Sbc	32.0	138	0.21	29.9	149	
	32.5	145	0.21	32.6		
7331	19.7	240	0.32	23.0	239	257
Sb	35.1	232	0.21	36.7	238	
	37.6	234	0.22	38.9		
2841	7.5	351	0.44	11.3	271	326
Sb	37.6	295	0.19	42.6	294	
	53.1	288	0.17	55.0		
5371	16.4	224	0.68	22.3	234	242
Sb	24.2	207	0.83	40.5	213	
	30.5	188	1.00	40.5		
2403	9.4	110	0.46	8.4	128	136
Sc	23.2	119	0.16	19.5	134	
6503	6.2	100	0.54	5.3	116	121
Sc	24.2	108	0.13	22.2	115	
2903	11.6	186	0.51	11.7	196	216
Sc	22.6	184	0.28	24.2	180	
5033	20.2	182	0.76	18.3	222	225
Sbc	36.7	182	0.49	35.4	200	

3. The action

Using Eq. (5), it is easy to see that for virialized systems the pair ($R_{\rm eff}$,$V_{\rm eff}$) univocally determines other pairs of dynamical parameters, such as ($R_{\rm eff}$,M), (M,$E_{\rm P}$) and (M, A), where in the last pair A is the action. The action is defined by

$$A = M R_{\rm eff} V_{\rm eff} \quad (9)$$

and has the same dimensionality of the angular momentum. But, contrary to the angular momentum, the action does not characterize the state of global rotation of the system. However, for a gravitating body, the action remains invariant during the prevalence of virial equilibrium. If this body presents the regime of

virial oscillations described by Ferronsky et al. (1987), A has the same value in the extremes of its Jacobi function (see the Appendix B). Then, we reinterpret the analysis of Campos-Aguilar et al. (1993) of spiral galaxies in a diagram of maximum rotational velocity $v_{\omega,\max}$ versus photometric radius R_{25}, which was considered equivalent to the classical angular momentum versus mass diagram. They found that, for a given mass, Sc galaxies have larger angular momentum ($\sim 20\%$) than Sa, in agreement with the Brosche's (1971) suggestion of the Hubble sequence as a sequence of angular momentum for a constant mass. In Fig. 2 we see that the peak values of the rotational velocity, $v_{\omega,\max}$, also do not differ significantly from $V_{\rm eff}$. With Eq. (7), this allows us to associate the pair (R_{25},$v_{\omega,\max}$) to ($R_{\rm eff}$,$V_{\rm eff}$) in the dynamical characterization of the "visible" galaxy, i.e. the part of galaxy inside R_{25}. As the pair ($R_{\rm eff}$,$V_{\rm eff}$) is equivalent to (M, A), in the analysis of Campos-Aguilar et al. (1993) the angular momentum can be replaced by the action. When we observe in our models of spiral galaxies a relatively large portion of non-rotational motions inside R_{25} through the rotational fraction of kinetic energy, ξ, in Table 1, this replacement is physically more sound.

Appendix A: the potential energy

A spiral galaxy modeled by disk, bulge and halo has the potential energy

$$E_{\rm P} = U_{\rm d} + U_{\rm b} + U_{\rm h} + U_{\rm bd} + U_{\rm hd} + U_{\rm bh}, \tag{A1}$$

where the three first terms of the right side are individual energies and the three last terms are due to interaction between the components.

The potential energy of a zero-thickness disk characterized by a superficial mass density $\Sigma_{\rm d}(R)$ is

$$U_{\rm d} = \pi \int_0^\infty \Phi_{\rm d}(R,0)\Sigma_{\rm d}(R) R\,{\rm d}R, \tag{A2}$$

being the disk potential in the plane $z = 0$ given by

$$\Phi_{\rm d}(R,0) = \int_0^\infty S(k) J_0(kR){\rm d}k, \tag{A3}$$

where

$$S(k) = -2\pi G \int_0^\infty J_0(kR)\Sigma_{\rm d}(R) R\,{\rm d}R \tag{A4}$$

and J_0 is the cylindrical Bessel function of order zero (Binney & Tremaine 1987, p. 76).

For a simple exponential disk, $\Sigma_{\rm d}(R) = \Sigma_0 \exp(-R/h)$, and we have $U_{\rm d} \approx -11.6 G\Sigma_0^2 h^3$.

If the bulge is modeled by a Hernquist sphere (Hernquist 1990) and if we truncate it at $r = r_{\rm t}$, its radial profile of mass density turns out to be

$$\rho_{\rm b}(r) = \frac{M_{\rm b}}{2\pi}\frac{(r_{\rm t}+c)^2}{r_{\rm t}^2}\frac{c}{r}\frac{1}{(r+c)^3} \tag{A5}$$

(if there is no truncation, $r_{\rm t} \to \infty$ in the expression above), giving the potential

$$\Phi_{\rm b}(r) = -GM_{\rm b}\frac{(r_{\rm t}+c)^2}{r_{\rm t}^2}\Big[\frac{1}{r+c} - \frac{c}{(r_{\rm t}+c)^2}\Big] \tag{A6}$$

for $r \le r_{\rm t}$, and

$$\Phi_{\rm b}(r) = -\frac{GM_{\rm b}}{r} \tag{A7}$$

for $r \ge r_{\rm t}$.

The potential energy of a spherical body is

$$U = -4\pi G \int_0^\infty M(r)\rho(r) r\,{\rm d}r. \tag{A8}$$

where $M(r)$ is the mass inside the radius r.

The density profile relative to Eq. (A5) yields to our bulge

$$M_{\rm b}(r) = M_{\rm b}\frac{(r_{\rm t}+c)^2}{r_{\rm t}^2}\frac{r^2}{(r+c)^2}, \tag{A9}$$

which results in

$$U_{\rm b}(r) = -\frac{GM_{\rm b}^2}{6c}\frac{(r_{\rm t}+c)^4}{r_{\rm t}^4}\Big[1 - \frac{c^2(3r_{\rm t}+c)}{(r+c)^3}\Big] \tag{A10}$$

A dark matter halo which extends to $r = r_{\rm m}$, modeled by

$$\rho_{\rm h}(r) = \frac{\rho_0}{1+(r/a)^2} \tag{A11}$$

gives the potential

$$\Phi_{\rm h}(r) =$$

$$-\frac{4\pi G\rho_0 a^3}{r}\left[\frac{r}{a} - \arctan\frac{r}{a} + \frac{r}{2a}\ln\Big(\frac{r_{\rm m}^2+a^2}{r^2+a^2}\Big)\right] \tag{A12}$$

for $r \le r_{\rm m}$, and the cumulative mass

$$M_{\rm h}(r) = 4\pi\rho_0\Big(\frac{r}{a} - \arctan\frac{r}{a}\Big). \tag{A13}$$

Using Eqs. (A11) and (A13) in Eq. (A8), this last equation can be numerically integrated to $r = r_{\rm m}$, giving $U_{\rm h}$.

The interactive terms of potential energy are

$$U_{\rm bd} = 2\pi \int_0^{r_{\rm m}} \Phi_{\rm b}\Sigma_{\rm d} R\,{\rm d}R, \tag{A14}$$

$$U_{\rm hd} = 2\pi \int_0^{r_{\rm m}} \Phi_{\rm h}\Sigma_{\rm d} R\,{\rm d}R, \tag{A15}$$

$$U_{\rm bh} = 4\pi \int_0^{r_{\rm m}} \Phi_{\rm b}\rho_{\rm h} r^2\,{\rm d}r \tag{A16}$$

and they also can be obtained by numerical integration.

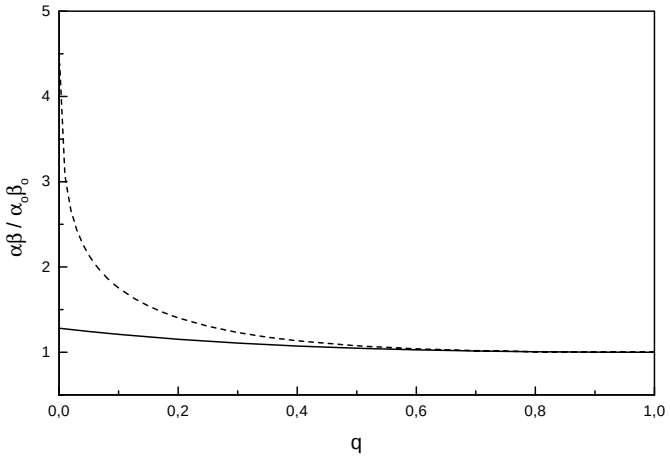

Fig. B1. Dependence of the product $\alpha\beta$ with the axial ratio q for oblate (solid line) and prolate (dashed line) spheroids.

Appendix B: the action in Jacobi dynamics

The Jacobi virial equation gives important informations about the global dynamics of a gravitational system. It is expressed by

$$\mathrm{d}^2\Phi/\mathrm{d}t^2 = 2E_\mathrm{K} + E_\mathrm{P}, \tag{B1}$$

being Φ the Jacobi function, namely,

$$\Phi = \frac{1}{2}\int \rho r^2 \mathrm{d}^3(r). \tag{B2}$$

The condition $\mathrm{d}^2\Phi/\mathrm{d}t^2 = 0$ is known as virial theorem and it does not determine a *static* equilibrium. If the Jacobi function of a virialized system evolves ($\mathrm{d}\Phi/\mathrm{d}t = constant \neq 0$) with constant total mechanical energy $E = E_\mathrm{K} + E_\mathrm{P}$ and constant mass, it is easy to see from Eqs. (1) and (2) and virial theorem condition that the parameters V_eff and R_eff do not change. Consequently, A does not change, either.

For a regime of oscillations around the virial equilibrium, a conservative global parameter also can be associated with A. By setting

$$-E_\mathrm{P} = \alpha\frac{GM^2}{R} \tag{B3}$$

and

$$\Phi = \frac{1}{2}M\beta^2R^2, \tag{B4}$$

where R is the radius of the system and α, β are dimensionless factors which depend of the internal mass distribution, we have

$$-E_P\sqrt{\Phi} = \frac{1}{\sqrt{2}}\alpha\beta GM^{5/2}. \tag{B5}$$

Ferronsky et al. (1987) found that for a great variety of spherically symmetrical mass distributions the product $\alpha\beta$ is nearly invariant around 0.5 and this invariance lead to unharmonic oscillations of the Jacobi function. If α_0 and β_0 refer to a spherical system, the flattening which transforms such a sphere into an oblate spheroid of semi-major axis R, in Eqs. (B3) and (B4), and semi-minor axis c results in

$$\alpha = \alpha_0\frac{\arcsin e}{e} \tag{B6}$$

and

$$\beta = \beta_0\Big(1 - \frac{e^2}{3}\Big)^{1/2}, \tag{B7}$$

where $e = \big[1-(c/R)^2\big]^{1/2}$ is the eccentricity. Now, a prolate spheroid with R and c defined as above has

$$\alpha = \alpha_0\frac{1}{2e}\ln\Big(\frac{1+e}{1-e}\Big) \tag{B8}$$

and

$$\beta = \beta_0\Big(1 - \frac{2e^2}{3}\Big)^{1/2}. \tag{B9}$$

In Fig. B1 the dependence of the product $\alpha\beta$ from the axial ratio $q = c/R$ of a spheroid is presented for both oblate and prolate cases. We see that the nearly invariance of $\alpha\beta$ can be extended even to highly eccentrical oblate spheroids and, consequently, also to hibrid systems formed by sphere or oblate spheroid and disk, but not to highly eccentrical prolate spheroids.

Defining the *generalized* action by

$$A_g \equiv \frac{1}{\alpha\beta}\Big[4E_\mathrm{K}\Phi - (\frac{\mathrm{d}\Phi}{\mathrm{d}t})^2\Big]^{1/2}, \tag{B10}$$

the use of Eq. (B1) yields

$$(\alpha\beta)^2\frac{\mathrm{d}A_g^2}{\mathrm{d}t} = 4\Phi\frac{\mathrm{d}E_\mathrm{K}}{\mathrm{d}t} - 2E_\mathrm{P}\frac{\mathrm{d}\Phi}{\mathrm{d}t}. \tag{B11}$$

In the last term of Eq. (B11), the invariance of the product $\alpha\beta$ gives

$$E_\mathrm{P}\frac{\mathrm{d}\Phi}{\mathrm{d}t} = -2\Phi\frac{\mathrm{d}E_\mathrm{P}}{\mathrm{d}t} \tag{B12}$$

which results in

$$(\alpha\beta)^2\frac{\mathrm{d}A_g^2}{\mathrm{d}t} = 4\Phi\frac{\mathrm{d}E}{\mathrm{d}t}. \tag{B13}$$

Then, we obtained the conservation of generalized action ($\mathrm{d}A_g/\mathrm{d}t = 0$) for a non- dissipative system ($\mathrm{d}E/\mathrm{d}t = 0$). While the conservation of angular momentum is interpreted through variational principle as a consequence of spatial rotational symmetry (Landau & Lifshitz 1976), the conservation of A_g is allowed by certain symmetry in the internal mass distribution.

Now, Eq. (B10) turns out

$$A_g = \frac{1}{\alpha\beta}\Big[(\alpha\beta)^2M^2R_\mathrm{eff}^2V_\mathrm{eff}^2 - (\frac{\mathrm{d}\Phi}{\mathrm{d}t})^2\Big]^{1/2} \tag{B14}$$

by the use of Eqs. (B4) and (B3) and results in Eq. (9) when $\mathrm{d}\Phi/\mathrm{d}t = 0$. Consequently,

$$A(\Phi_\mathrm{max}) = A(\Phi_\mathrm{min}) = A_g. \tag{B15}$$

References

Begeman K., 1987, Ph. D. Thesis. University of Groningen
Binney J.J., Tremaine,S., 1987, Galactic Dynamics, Princeton Univ. Press, Princeton
Brosche P., 1971, A&A 13, 293
Campos-Aguilar A., Prieto M., Garcia C., 1993, A&A 276, 16
Casertano S., 1983, MNRAS 203, 735
Ferronsky V.I., Denisik S.A., Ferronsky S.V., 1987, Jacobi Dynamics. D. Reidel, Dordrecht
Hernquist L., 1990, Ap J 356, 359
Landau L., Lifshitz E., 1976, Mechanics, 3rd ed., Pergamon, Oxford